A Lagrangian alternative to ΛCDM and fit to cosmological data

DSU2024, Corfu, Greece

September 8-14, 2024

PN

Northeastern University, Boston, Massachusetts, USA.

September 8-14, 2024

Topics[1]

See also talk by Eleonora Di Valentino

- $\boldsymbol{\Lambda}$CDM is enormously successful (aside from some anomalies) but is based on a fluid model which has no simple field theoretic basis.
- In this talk we provide a field theoretic alternative to $\boldsymbol{\Lambda}$CDM.
- For specificity we will discuss an explicit model of interacting dark matter and dark energy ($\boldsymbol{\mathcal{L}}$dmde), and compute density perturbations and velocity divergence perturbations within a field theoretic formalism.
- We will then carry out numerical fits to the cosmological data which includes data from Planck (with lensing), BAO, Pantheon, SH0ES, and WiggleZ, and specifically discuss $\boldsymbol{H_0}$ and $\boldsymbol{S_8}$ tensions.
- Conclusions

[1] Talk based on: A. Aboubrahim and P.N., [arXiv:2406.19284 [astro-ph.CO]].

$\mathbf{\Lambda}$CDM model

- The $\mathbf{\Lambda}$CDM is based on fluid equations of motion

$$\boldsymbol{\mathcal{D}_\alpha T_\phi^{\alpha\beta} = J_\phi^\beta}, \quad \boldsymbol{(DE)}$$
$$\boldsymbol{\mathcal{D}_\alpha T_\chi^{\alpha\beta} = J_\chi^\beta}, \quad \boldsymbol{(DM)}$$

  with the constraint $\boldsymbol{J_\phi^\beta = -J_\chi^\beta}$ which is introduced in an ad hoc manner.

- One the other hand all the fundamental theories of physics are based on Lagrangians and an action principle. This includes the standard model, Einstein theory, string theory. So the $\mathbf{\Lambda}$CDM concordance model cannot be considered as a fundamental cosmological model.

- In this talk I will discuss a field theoretic Lagrangian formulation of dark matter (DM) and dark energy (DE) ($\boldsymbol{\mathcal{L}}$dmde) as an alternative to $\mathbf{\Lambda}$CDM.

- **We will use a specific model of DM and DE as an illustrative example but the underlying formalism is valid for any field theoretic choice of DM and DE.**

An illustrative example of $\mathcal{L}$dmde

A Lagrangian formulation of interacting two spin zero DM and DE fields

$$A = \int \mathrm{d}^4 x \sqrt{-g} \left[-\frac{1}{2} \phi^{,\mu} \phi_{,\mu} - \frac{1}{2} \chi^{,\mu} \chi_{,\mu} - V(\phi, \chi) \right],$$

$$\begin{aligned}
V(\phi,\chi) &= V_1(\chi) + V_2(\phi) + V_3(\phi,\chi), \\
V_1(\chi) &= \frac{1}{2} m_\chi^2 \chi^2 + \frac{\lambda}{4} \chi^4 && (DM) \\
V_2(\phi) &= \mu^4 \left[1 + \cos\left(\frac{\phi}{F}\right) \right] && (DE), \\
V_3(\phi,\chi) &= \frac{\tilde{\lambda}}{2} \chi^2 \phi^2, && (DM/DE \text{ interaction})
\end{aligned}$$

Background equations

For the background we consider a flat, homogeneous and isotropic universe characterized by the Friedmann-Roberston-Walker (FRW) metric.

$$\mathrm{d}s^2 = g_{\mu\nu}\mathrm{d}x^\mu \mathrm{d}x^\nu = a^2(-\mathrm{d}\tau^2 + \gamma_{ij}\mathrm{d}x^i \mathrm{d}x^j),$$

a is time-dependent scale factor; γ_{ij} are spatial components of the metric; and τ is conformal time so that $\mathrm{d}\tau = \mathrm{d}t/a(t)$.

KG equations

$$\chi_0'' + 2\mathcal{H}\chi_0' + a^2(\bar{V}_1 + \bar{V}_3)_{,\chi} = 0,$$
$$\phi_0'' + 2\mathcal{H}\phi_0' + a^2(\bar{V}_2 + \bar{V}_3)_{,\phi} = 0,$$

where $\bar{V}(\phi,\chi) \equiv V(\phi_0,\chi_0)$ and $\bar{V}_{1,\chi} \equiv (V_{1,\chi})_{\chi=\chi_0}$, etc; and $\mathcal{H} = aH$, and $H = \dot{a}/a$.

Continuity equations for the densities

Field theory model

$$\rho_\phi' + 3\mathcal{H}(1 + w_\phi)\rho_\phi = Q_\phi\,, \quad \text{DE}$$
$$\rho_\chi' + 3\mathcal{H}(1 + w_\chi)\rho_\chi = Q_\chi\,, \quad \text{DM}$$
$$\rho' + 3\mathcal{H}(1 + w)\rho = 0, \quad \text{(energy conservation)}$$
$$\rho = \rho_\phi + \rho_\chi - V_3$$
$$Q_\phi = \bar{V}_{3,\chi}\chi', \quad Q_\chi = \bar{V}_{3,\phi}\phi'.$$

ΛCDM model: In this model one sets $Q_\phi = -Q_\chi = Q$ to guarantee energy conservation. The constraint $Q_\phi = -Q_\chi$ is ad hoc.

$$\rho_\phi' + 3\mathcal{H}(1 + w_\phi)\rho_\phi = Q\,, \quad \text{DE}$$
$$\rho_\chi' + 3\mathcal{H}(1 + w_\chi)\rho_\chi = -Q\,. \quad \text{DM}$$

Linear perturbations

Linear perturbations around the background involve perturbation of the spin zero fields and of the metric

$$\chi(t,\vec{x}) = \chi_0(t) + \chi_1(t,\vec{x}) + \cdots\,, \quad \phi(t,\vec{x}) = \phi_0(t) + \phi_1(t,\vec{x}) + \cdots$$

Perturbations of the metric in a general gauge

$$\begin{cases} g^{00} = -a^{-2}(1-2A), \\ g^{0i} = -a^{-2}B^i, \\ g^{ij} = a^{-2}(\gamma^{ij} - 2H_L\gamma^{ij} - 2H_T^{ij}), \end{cases}$$

A is a scalar potential, B^i a vector shift, H_L is a scalar perturbation to the spatial curvature and H_T^{ij} is a trace-free distortion to the spatial metric.

Synchronous and conformal (Newtonian) gauges

Synchronous gauge:

In this gauge

$$A = B = 0,$$
$$H_L = \frac{1}{6}h,$$

h is trace of the metric perturbations h_{ij}.

Conformal (Newtonian) gauge:

This gauge is characterized by

$$B = H_T = 0,$$
$$A \equiv \Psi$$
$$H_L \equiv \Phi$$

We will carry out our calculations in the general gauge and then present our final results in the synchronous and conformal gauges based on the above prescription.

Perturbation of the stress-energy tensor

The perturbed object is

$$T^{\mu}_{\nu} = \bar{T}^{\mu}_{\nu} + \delta T^{\mu}_{\nu}$$

$$\begin{aligned}
T^0_0 &= -\rho - \delta\rho \\
T^0_i &= (\rho + p)(v_i - B_i) \\
T^i_0 &= -(\rho + p)v_i \\
T^i_j &= (p + \delta p)\delta^i_j + p\Pi^i_j,
\end{aligned}$$

with Π^i_j representing the anisotropic stress, v_i the 3-velocity, $\delta\rho$ and δp being the density and pressure perturbations.

Velocity divergence: θ/Θ

Computation of the perturbed off-diagonal element δT^0_i gives

$$\delta T^0_i = -a^{-2}\phi_0'\delta\phi_{,i}.$$

In Fourier space, we can define velocity divergence $\theta = ik^i v_i$ or alternately $\Theta \equiv (1+w)\theta$ which are determined by

$$\rho_\phi \Theta_\phi = \frac{k}{a^2}\phi_0'\phi_1,$$
$$\rho_\chi \Theta_\chi = \frac{k}{a^2}\chi_0'\chi_1\,.$$

First order perturbations of the KG equations

$$\phi_1'' + 2\mathcal{H}\phi_1' + (k^2 + a^2\bar{V}_{,\phi\phi})\phi_1 + a^2\bar{V}_{,\phi\chi}\chi_1 + 2a^2\bar{V}_{,\phi}A + (3H_L' - A' + kB)\phi_0' = 0,$$

$$\chi_1'' + 2\mathcal{H}\chi_1' + (k^2 + a^2\bar{V}_{,\chi\chi})\chi_1 + a^2\bar{V}_{,\chi\phi}\phi_1 + 2a^2\bar{V}_{,\chi}A + (3H_L' - A' + kB)\chi_0' = 0.$$

Density perturbations (contrasts)

$$\delta_i \equiv \frac{\delta\rho_i}{\bar{\rho}_i} = \frac{\rho_i(t,\vec{x}) - \bar{\rho}_i(t)}{\bar{\rho}_i},$$

Solving the KG equations can be computationally demanding when the time scale set by m_χ^{-1} becomes much smaller than the Hubble time $\mathcal{H}^{-1}$, i.e., $m_\chi^{-1} << \mathcal{H}^{-1}$ when the DM field starts its rapid oscillations. For this reason, it is more practical to turn these equations into differential equations in δ_i and Θ_i [2]

[2] M. S. Turner, "Coherent Scalar Field Oscillations in an Expanding Universe," Phys. Rev. D **28**, 1243 (1983).

First order equations for density perturbations and for velocity divergence [3]

For the DM field χ, we obtain a first order differential equation of the density contrast

$$\delta'_\chi = \left[3\mathcal{H}(w_\chi - c^2_{s\chi}) - \frac{Q_\chi}{\rho_\chi}\right]\delta_\chi + \frac{3\mathcal{H}Q_\chi}{\rho_\chi(1+w_\chi)}(c^2_{s\chi} - c^2_{\chi_{\rm ad}})\frac{\Theta_\chi}{k} - 9\mathcal{H}^2(c^2_{s\chi} - c^2_{\chi_{\rm ad}})\frac{\Theta_\chi}{k} - \Theta_\chi k$$
$$+ \frac{a^2}{k}\frac{\rho_\phi}{\rho_\chi}\bar{V}_{3,\phi\phi}\Theta_\phi + \frac{1}{\rho_\chi}\bar{V}_{3,\chi\phi}\phi'_0\chi_1 + \frac{1}{\rho_\chi}\bar{V}_{3,\phi}\phi'_1 - (3H'_L + kB)(1+w_\chi),$$

and for the velocity divergence

$$\Theta'_\chi = (3c^2_{s\chi} - 1)\mathcal{H}\Theta_\chi + k\delta_\chi c^2_{s\chi} + 3\mathcal{H}(w_\chi - c^2_{\chi_{\rm ad}})\Theta_\chi$$
$$- \frac{Q_\chi}{\rho_\chi}\left(1 + \frac{c^2_{s\chi} - c^2_{\chi_{\rm ad}}}{1+w_\chi}\right)\Theta_\chi + \frac{k}{\rho_\chi}\bar{V}_{3,\phi}\phi_1 + k(1+w_\chi)A.$$

Note that two types of sound speeds enter in the analysis: $c_{s\chi}$ and $c^2_{\chi_{\rm ad}}$ where $c_{s\chi}$ is defined so that

$$c^2_{s\chi} = \frac{\delta p_\chi}{\delta\rho_\chi}.$$

[3] A. Aboubrahim and P.N., [arXiv:2406.19284 [astro-ph.CO]].

Adiabatic sound speed $c^2_{\chi_{\rm ad}}$ and equation of state w_χ

Adiabatic sound speed is determined in part by the equation of state

$$c^2_{\chi_{\rm ad}} \equiv \frac{p'_\chi}{\rho'_\chi} = w_\chi - \frac{w'_\chi \rho_\chi}{3\mathcal{H}(1+w_\chi)\rho_\chi - Q_\chi}.$$

Equation of state for the DM field χ

$$w_\chi = \frac{\frac{3\lambda}{8m_\chi^4}\langle\rho_\chi\rangle}{1 + \frac{9\lambda}{8m_\chi^4}\langle\rho_\chi\rangle + \frac{\tilde{\lambda}\phi_0^2}{m_\chi^2}},$$

- $\lambda = 0$: When self-interactions are absent $w_\chi = 0$ and we have pressure-less fluid as in CDM.
- When $\frac{9\lambda}{8m_\chi^4}\langle\rho_\chi\rangle >> 1$, $w_\chi \to \frac{1}{3}$, which indicates a period where the would be matter field χ behaves as radiation. This is verified in numerical analysis.

Speed of sound in DM fluid

A lengthy calculation gives the speed of sound in the DM fluid

$$c_{s\chi}^2 = \frac{\left(\frac{k}{2m_\chi a}\right)^2 + \frac{3\lambda}{4m_\chi^4}\langle\rho_\chi\rangle}{1 + \left(\frac{k}{2m_\chi a}\right)^2 + \frac{9\lambda}{4m_\chi^4}\langle\rho_\chi\rangle + \frac{\tilde{\lambda}\phi_0^2}{m_\chi^2}}.$$

Numerical analysis and fits to cosmological data

The analysis consists of: Part I and Part II.

- Part I: We use a number of benchmarks to exhibit the effect of DM self-interaction, DM-DE coupling, and of the DM mass on the background and perturbation on observables.

  Input parameters:

  $$\mu, F, m_\chi, \lambda, \tilde{\lambda}; \quad \phi_{ini}, \phi'_{ini}; \chi_{ini}, \chi'_{ini}; a_{ini} \sim 10^{-14}.$$

  We evolve the background DM and DE fields and their perturbations using the Boltzmann solver `CLASS` [4]. Here we will investigate the effects of variations of $\lambda, \tilde{\lambda}, m_\chi$ on

  $$\delta_\chi, \; \Theta_\chi$$
  $$P(k), \frac{\ell(\ell+1)}{2\pi} C_\ell^{TT}$$
  $$H(z), w_\phi, w_\chi, \Omega_\phi, \Omega_\chi, \Omega_\gamma, \Omega_b, Q_\phi, Q_\chi$$

- Part II: We use MC Monte Carlo simulations to extract the cosmological parameters.

[4] D. Blas, J. Lesgourgues and T. Tram, JCAP **07**, 034 (2011), https://github.com/lesgourg/class_public.

Part I

The effect of dark matter self-interaction

A. Aboubrahim and P.N., [arXiv:2406.19284 [astro-ph.CO]]

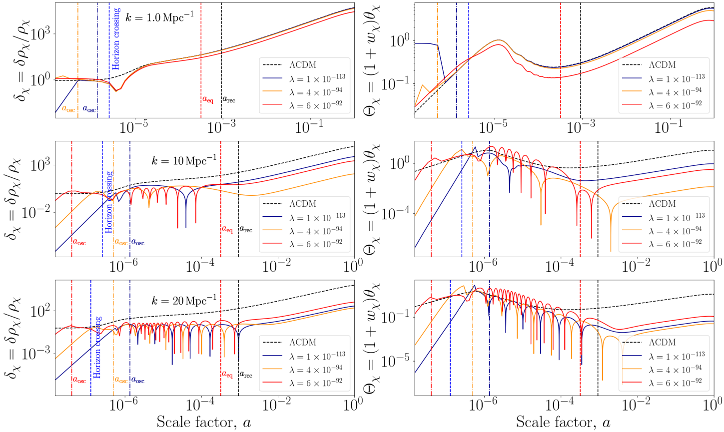

Fig.A: The three benchmarks representing three DM self-interaction strengths. Plots showing the DM density contrast (left) and the velocity divergence (right) as a function of the scale factor for three wave numbers $\boldsymbol{k}$. The three dotted vertical lines correspond to the time of horizon crossing (blue), matter-radiation equality (red) and recombination (black). The dash-dot vertical lines correspond to $\boldsymbol{a_{\mathrm{osc}}}$, the scale factor when oscillations of the field start.

The effect of dark matter self-interaction

A. Aboubrahim and P.N., [arXiv:2406.19284 [astro-ph.CO]]

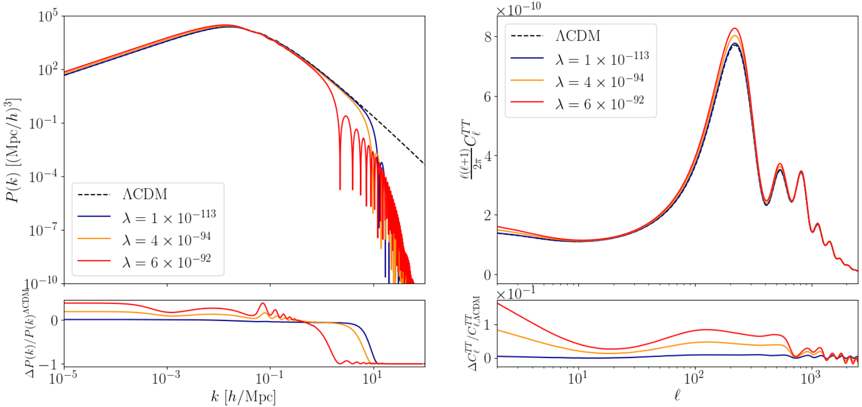

Fig.B: Left panel: the matter power spectrum plotted against the wavenumber for three DM interaction strengths. Right panel: the temperature TT power spectrum as a function of the multipoles also for three benchmarks representing three DM self-interaction strengths. The dashed line represents **Λ**CDM.

The effect of dark matter self-interaction

A. Aboubrahim and P.N., [arXiv:2406.19284 [astro-ph.CO]]

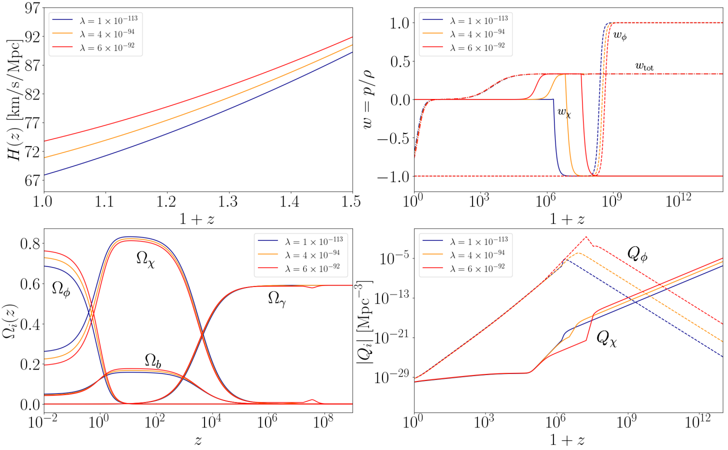

Fig.C: Upper row: plot of the Hubble parameter $\boldsymbol{H(z)}$ (left panel) and the DM EoS (solid), DE EoS (dashed) and the total EoS (dash-dot) (right panel) versus $\mathbf{1+z}$ for three $\boldsymbol{\lambda}$ benchmarks. Lower row: plots of the energy density fraction of DM, DE, baryons and radiation (left panel) and the couplings $\boldsymbol{Q_\chi}$ and $\boldsymbol{Q_\phi}$ (right panel) as a function of the redshift for three benchmarks of the self-interaction $\boldsymbol{\lambda}$

Effect of DM-DE interaction on DM density perturbations and on velocity divergence

A. Aboubrahim and P.N., [arXiv:2406.19284 [astro-ph.CO]]

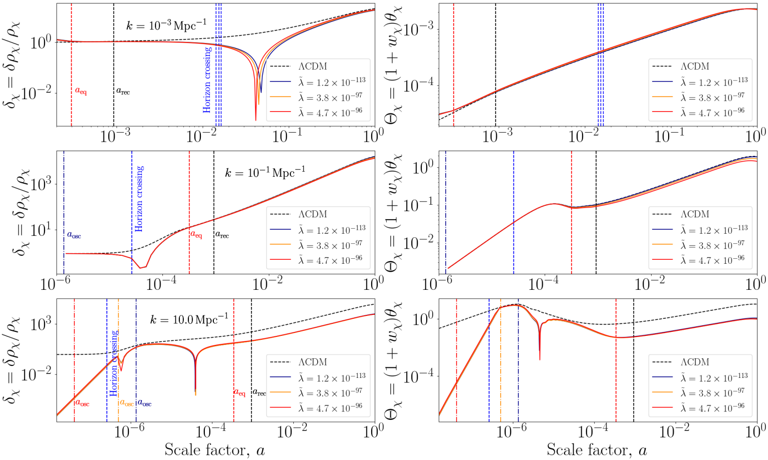

Fig. A1: Same as Fig. A except that the three benchmarks representing three DM-DE interaction strengths.

Effect of DM-DE interaction on power spectrum

A. Aboubrahim and P.N., [arXiv:2406.19284 [astro-ph.CO]]

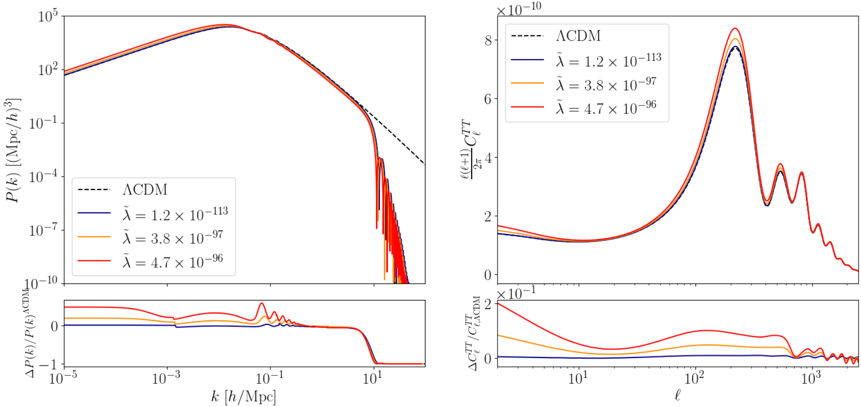

Fig. B1: Same as Fig. B except that the three benchmarks representing three DM-DE interaction strengths.

Effect of varying the DM mass

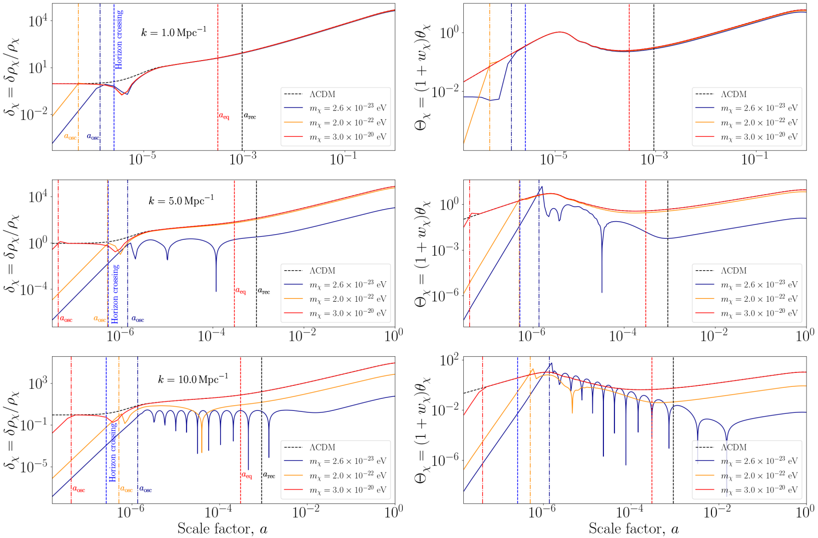

Fig. A2: Same as Fig. A except for the variation of the DM mass.

Effect of DM-DE interaction on cosmological evolution

A. Aboubrahim and P.N., [arXiv:2406.19284 [astro-ph.CO]]

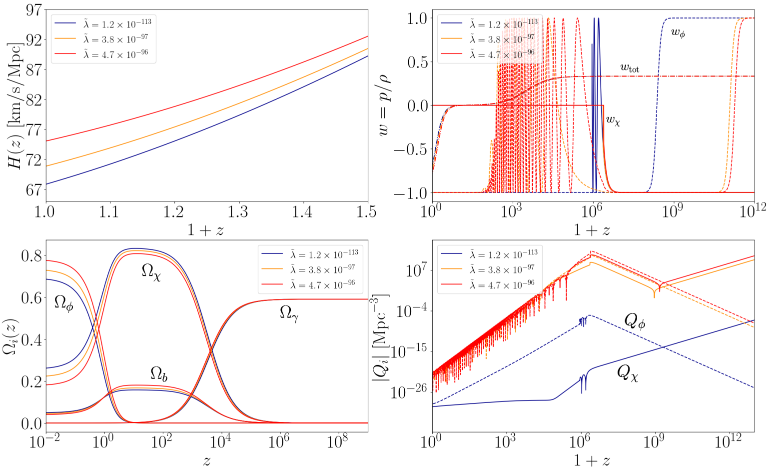

Fig. C1: Same as Fig. C except that the three benchmarks representing three DM-DE interaction strengths.

Effect of varying the DM mass

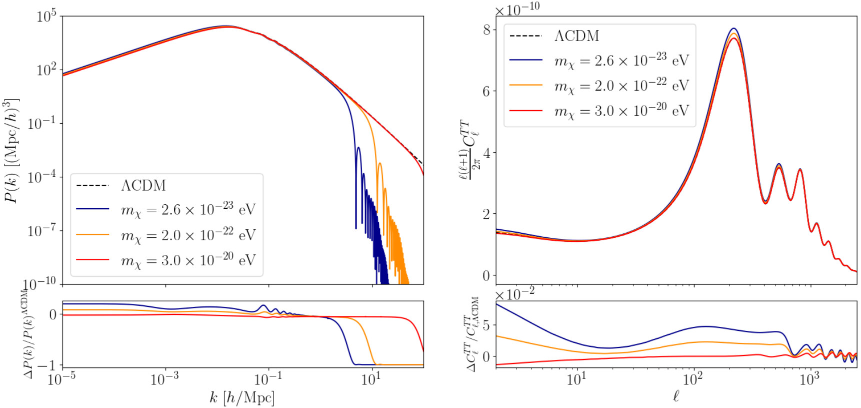

Fig. B2: Same as Fig. B except for the variation of the DM mass.

Effect of varying the DM mass

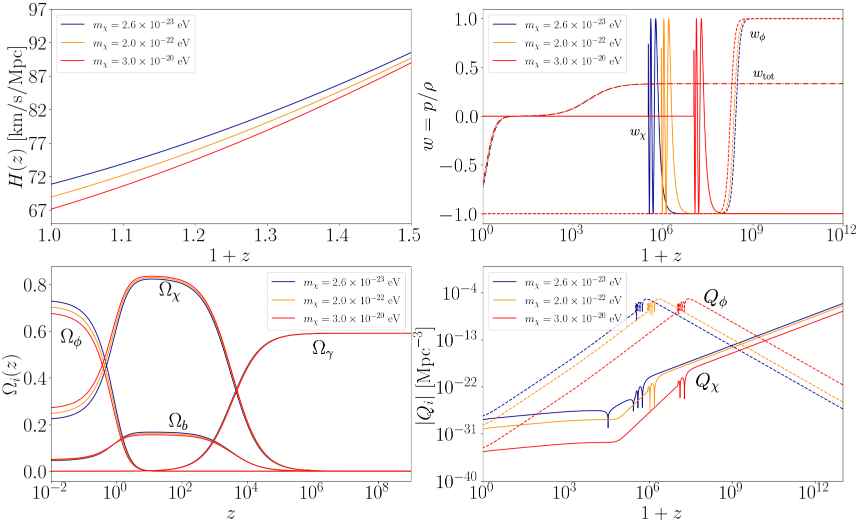

Fig C2: Same as Fig. C except for the variation of the DM mass.

Part II

Constraints from cosmological data

1. The Planck 2018 temperature anisotropies and polarization measurements [5]
2. The Planck 2018 lensing likelihood[6]
3. Baryon Acoustic Oscillation (BAO) data: [7]
4. The combination Pantheon+SH0ES [8]
5. WiggleZ survey[9]

---

[5] N. Aghanim *et al.* [Planck], Astron. Astrophys. **641**, A6 (2020); Astron. Astrophys. **641**, A5 (2020); Astron. Astrophys. **641**, A1 (2020).

[6] N. Aghanim *et al.* [Planck], Astron. Astrophys. **641**, A8 (2020).

[7] A. J. Ross *et al.* Mon. Not. Roy. Astron. Soc. **449**, no.1, 835-847 (2015);C. P. Ahn *et al.* [BOSS], Astrophys. J. Suppl. **203**, 21 (2012); S. Alam *et al.* [BOSS], Mon. Not. Roy. Astron. Soc. **470**, no.3, 2617-2652 (2017); S. Alam *et al.* [eBOSS], Phys. Rev. D **103**, no.8, 083533 (2021); C. Howlett*et al.* Mon. Not. Roy. Astron. Soc. **449**, no.1, 848-866 (2015); F. Beutler *et al.* Mon. Not. Roy. Astron. Soc. **416**, 3017-3032 (2011).

[8] D. Brout **416** Astrophys. J. **938**, no.2, 110 (2022); A. G. Riess *et al.* Astrophys. J. Lett. **934**, no.1, L7 (2022).

[9] D. Parkinson *et al.* Phys. Rev. D **86**, 103518 (2012) .

Summary of our MCMC analysis

Next we do a MCMC fit to the cosmological data in 5 different combinations. We look for best fits to the cosmological parameters: $\boldsymbol{H_0, \Omega_m, \Omega_\phi, \sigma_8, S_8}$.

To check the goodness of the fits we define: $\boldsymbol{\Delta\chi^2_{\text{min}} = \chi^2_{\text{min},\mathcal{L}\text{dmde}} - \chi^2_{\text{min},\Lambda\text{CDM}}}$.

Result of $\mathcal{L}$dmde analysis

Data sets	$\boldsymbol{\Delta\chi^2_{\text{min}}}$
Planck + BAO:	**(0.0)**
Planck+ Lensing:	**(0.0)**
Planck + Pantheon + SHOES	**(−1.0)**
Planck+ Lensing + BAO+ WiggleZ	**(+1.0)**
All	**(−1.0)**

- The first two data sets show no difference between $\mathcal{L}$dmde and ΛCDM.
- The third data set and the combination of all data show that the $\mathcal{L}$dmde fits the data better, although only slightly.

MCMC analysis for interacting dark matter-dark energy ($\mathcal{L}$dmde) model

Parameter	Planck +BAO	Planck +Lensing	Planck+Pantheon +SH0ES	Planck+Lensing +BAO+WiggleZ	ALL
$100\Omega_b h^2$	2.243 ± 0.014	2.238 ± 0.015	2.265 ± 0.014	2.250 ± 0.014	2.266 ± 0.014
$\Omega_\chi h^2$	0.1192 ± 0.0010	0.1199 ± 0.0012	0.1169 ± 0.0011	0.1184 ± 0.0009	0.1170 ± 0.0008
$100\theta_s$	1.0419 ± 0.0003	1.0419 ± 0.0003	1.0419 ± 0.0003	1.0419 ± 0.0003	1.0420 ± 0.0003
$10^{-2} \ln \lambda$	< -2.2	< -2.2	< -2.2	< -2.2	< -2.2
$10^{-2} \ln \tilde{\lambda}$	< -2.33	< -2.33	< -2.33	< -2.33	< -2.33
$\ln m_\chi$	> -43.6	> -43.64	> -43.58	> -43.81	> -43.72
H_0	$67.73^{+1.80}_{-0.52}$	$67.40^{+2.40}_{-0.08}$	$68.84^{+2.10}_{-0.24}$	$68.10^{+1.80}_{-0.48}$	$68.81^{+1.60}_{-0.67}$
$\Omega_{\rm m}$	$0.3102^{+0.0077}_{-0.0092}$	$0.315^{+0.013}_{-0.012}$	$0.296^{+0.012}_{-0.008}$	$0.3052^{+0.0086}_{-0.0079}$	$0.2963^{+0.0062}_{-0.0094}$
Ω_ϕ	$0.6897^{+0.0230}_{-0.0007}$	$0.685^{+0.031}_{-0.003}$	$0.704^{+0.025}_{-0.000}$	$0.6948^{+0.0229}_{-0.0008}$	$0.7036^{+0.0200}_{-0.0040}$
σ_8	$0.8086^{+0.0350}_{-0.0010}$	$0.8103^{+0.0250}_{-0.0021}$	$0.803^{+0.040}_{-0.011}$	$0.8061^{+0.0329}_{-0.0034}$	$0.8043^{+0.0280}_{-0.0006}$
S_8	$0.822^{+0.014}_{-0.032}$	$0.829^{+0.016}_{-0.028}$	$0.7975^{+0.0180}_{-0.0250}$	$0.813^{+0.028}_{-0.031}$	$0.7993^{+0.0410}_{-0.0140}$
$\Delta\chi^2_{\rm min}$	0.0	0.0	-1.0	$+1.0$	-1.0

Table 2: Constraints on some of the cosmological parameters of our model. The values are quoted at 68% CL intervals, unless an upper or lower bounds are shown, in which case it is the 95% CL interval. The lowermost row shows $\Delta\chi^2_{\rm min} = \chi^2_{\rm min,iDMDE} - \chi^2_{\rm min,\Lambda CDM}$, where iDMDE stands for our interacting dark matter-dark energy model.

- $\boldsymbol{H_0}$ tension

Planck	$\boldsymbol{H_0^{\mathrm{Pl}} = (67.4 \pm 0.5)}$km/s/Mpc
SHOES	$\boldsymbol{H_0^{\mathrm{R22}} = (73.04 \pm 1.04)}$km/s/Mpc
$\mathcal{L}$dmde	$\boldsymbol{H_0 = (68.84^{+2.10}_{-0.24})}$ km/s/Mpc

The $\boldsymbol{H_0}$ tension is more than $\boldsymbol{5\sigma}$. The $\mathcal{L}$dmde$\boldsymbol{H_0}$ is now $\boldsymbol{\sim 2.7\sigma}$ away from the R22 measurement indicating a slight improvement in reducing tension.

- $\boldsymbol{S_8}$ tension.

Planck	$\boldsymbol{S_8^{\mathrm{Pl}} = 0.834 \pm 0.016}$
KiDS-1000	$\boldsymbol{S_8^{\mathrm{KiDS}} = 0.759^{+0.024}_{-0.021}}$
DES-Y3	$\boldsymbol{S_8^{\mathrm{DES}} = 0.759^{+0.025}_{-0.023}}$
$\mathcal{L}$dmde	$\boldsymbol{S_8 = 0.7975^{+0.0180}_{-0.0250}}$

Thus $\mathcal{L}$dmde value(using the Planck + Pantheon + SHOES data sets) is consistent with both KiDS and DES [10] and resolves the $\boldsymbol{\sim 3\sigma}$ tension that $\boldsymbol{S_8}$ has with the Standard Model. A similar result in resolving the $\boldsymbol{S_8}$ tension is based on including a drag term between DM and DE [11]

[10]. M. Asgari *et al.* [KiDS], Astron. Astrophys. **645**, A104 (2021).
A. Amon *et al.* [DES], Phys. Rev. D **105**, no.2, 023514 (2022); L. F. Secco *et al.* [DES], Phys. Rev. D **105**, no.2, 023515 (2022).

[11] V. Poulin, J. L. Bernal, E. D. Kovetz and M. Kamionkowski, Phys. Rev. D **107**, no.12, 123538 (2023).

Conclusion

- The $\mathbf{\Lambda}$CDM model is based on fluid equations. It is not motivated by an underlying Lagrangian and is not at the same footing as the standard model of particle physics or Einstein gravity.
- We have discussed an alternative approach, i.e., $\boldsymbol{\mathcal{L}}$dmde, which is field theoretic and produces a consistent set of Lagrangian equations which replace the fluid equations of $\mathbf{\Lambda}$CDM. The $\boldsymbol{\mathcal{L}}$dmde provides the proper framework for cosmological analyses.
- We have carried out fits to the cosmological data using $\boldsymbol{\mathcal{L}}$dmdeand find $\boldsymbol{\chi^2}$ fits to the data at the same level as the $\mathbf{\Lambda}$CDM.
- The field theoretic model is theoretically robust and with more data we should be able to either resolve the tensions or point to the possibility of new physical phenomena related to the tensions.

Extra slides

Recent DESI result: arXiv-2404.03002

- DESI paper arXiv-2404.03002 makes measurements of baryon acoustic oscillations (BAO) in galaxy, quasar and Lyman-α forest in the range of $0.1 < z < 4.2$. Combining with CMB data they find

$$\Omega_m = 0.307 \pm 0.005, \quad H_0 = (67.97 \pm 0.38)\mathrm{kms}^{-1}\mathrm{Mpc}^{-1}.$$

$$w = -0.99^{+0.15}_{-0.13}$$

- The result on w has been interpreted that the DESI analysis might be indication of a time varying quintessence field. Typically w for a time-varying dark energy is parametrized so that

$$w(z) = w_0 + w_a \frac{z}{1+z}$$

But this parametrization is valid only for low z and does and not applicable at any z. Specifically if $w = w_0 + w_a < -1$ is indicated by data, it does not mean phantom energy which violates the Null Energy Condition which is[12]:

$$T_{\mu\nu} k^\mu k^\nu \geq 0.$$

[12] David Shlivko and Paul J. Steinhardt: 2405.03933[astro-ph.CO].

Analysis with Planck, BAO, Pantheon, WiggleZ data

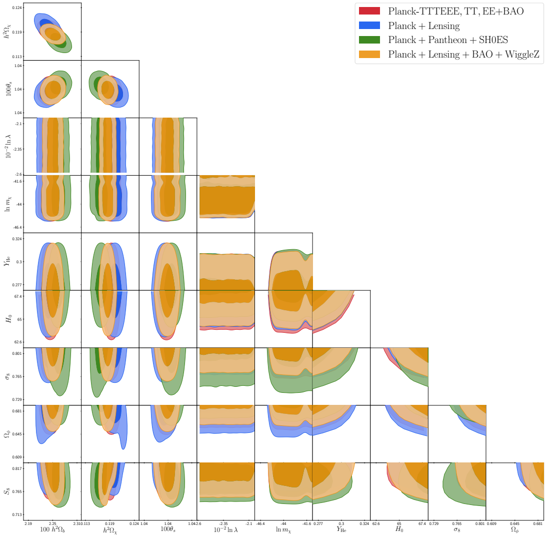

Fig.10: The triangular posterior distributions of some of our model cosmological parameters for a combination of datasets shown in the figure legend. For each dataset, we show the allowed regions at 68% and 95% CL.

Constraints on $\boldsymbol{\lambda}$, $\tilde{\boldsymbol{\lambda}}$, $\boldsymbol{m_\chi}$

We also set upper limits on the DM self-interaction strength $\boldsymbol{\lambda}$ and the DM-DE interaction strength $\tilde{\boldsymbol{\lambda}}$ at 95% CL, and we set a lower limit on the mass of an ultralight DM scalar field constituting all of the DM density today

$$\boldsymbol{\lambda} \leq \mathbf{2.85 \times 10^{-96}},$$
$$\tilde{\boldsymbol{\lambda}} \leq \mathbf{6.45 \times 10^{-102}},$$
$$\boldsymbol{m_\chi} \geq \mathbf{1.03 \times 10^{-19}}\mathrm{eV}.$$

Density perturbation δ_ϕ in the conformal gauge is given by

$$\delta'_\phi = \left[3\mathcal{H}(w_\phi - c_\phi^2) - \frac{Q_\phi}{\rho_\phi}\right]\delta_\phi + \frac{3\mathcal{H}Q_\phi}{\rho_\phi(1+w_\phi)}(c_\phi^2 - c_{\phi_{\mathrm{ad}}}^2)\frac{\Theta_\phi}{k} - 9\mathcal{H}^2(c_\phi^2 - c_{\phi_{\mathrm{ad}}}^2)\frac{\Theta_\phi}{k} - \Theta_\phi k$$
$$+ \frac{a^2}{k}\frac{\rho_\chi}{\rho_\phi}\bar{V}_{3,\chi\chi}\Theta_\chi + \frac{1}{\rho_\phi}\bar{V}_{3,\phi\chi}\chi'_0\phi_1 + \frac{1}{\rho_\phi}\bar{V}_{3,\chi}\chi'_1 + 3\Psi'(1+w_\phi), \quad (1)$$

The velocity divergence Θ_ϕ in the conformal gauge is given by

$$\Theta'_\phi = (3c_\phi^2 - 1)\mathcal{H}\Theta_\phi + k\delta_\phi c_\phi^2 + 3\mathcal{H}(w_\phi - c_{\phi_{\mathrm{ad}}}^2)\Theta_\phi$$
$$- \frac{Q_\phi}{\rho_\phi}\left(1 + \frac{c_\phi^2 - c_{\phi_{\mathrm{ad}}}^2}{1+w_\phi}\right)\Theta_\phi + \frac{k}{\rho_\phi}\bar{V}_{3,\chi}\chi_1 + k(1+w_\phi)\Psi, \quad (2)$$